Proceedings of the 32nd Conference
on Decision and Control
San Antonio, Texas • December 1993

Sliding Mode Control for an Obstacle Avoidance Strategy Based on an Harmonic Potential Field

Jürgen Guldner * Vadim I. Utkin †

DLR, German Aerospace Research Establishment
Institute for Robotics and System Dynamics
Postfach 1116, 82230 Wessling, Germany
email: df68@master.df.op.dlr.de

*Author to whom all correspondance should be addressed.
†Currently on leave from the Institute of Control Sciences, Moscow, Russia.

Abstract

This paper introduces a new integrated path control strategy (combined path planning and motion control) for autonomous systems of arbitrary dimension. A harmonic artificial potential field is used to specify admissible trajectories leading around obstacles. Using a sliding mode controller, motion is generated *along* the gradient lines of the potential field, avoiding collisions with the obstacles. The extremely low computational complexity of the proposed method makes it very suitable for on-line applications. The strategy is applied to mobile robots moving amidst known obstacles. Only the obstacle closest to the robot is considered at each time instance. The switching of the two respective gradient fields along the equi-distance line between two obstacles leads to the interesting phenomenon of an additional "spatial" sliding surface, which is examined in detail. The algorithm guarantees approaching the goal point continuously, following a reasonably short path. Numerical examples are presented to demonstrate the utility of this new strategy.

1 Introduction

Path control for autonomous mechanical systems ususally is devided into two subtasks, path planning and motion control, both incorporated in different levels of the control hierarchy. The task "path planning" is to determine a collision-free path (possibly optimizing pathlength, control effort along the path, etc.) at one of the higher control levels. The task "motion control" utilizes a low level controller to provide motion along the desired path.

The path planning approaches can be categorized into *global* and *local* strategies. Global strategies are based on global a priori information of the entire workspace. Since the time cycle of the higher control level, which is usually several orders of magnitude slower than the lower levels and the system responses, dictates the speed of operation, global approaches are often impractical for on-line applications in partially known or changing environments. Local methods, on the other hand, assume incomplete knowledge of the environment and guide the motion based on local information acquired by sensors (vision, ultra-sound, etc.).

Recently, researchers tried to combine the advantages of both approaches in an attempt to remedy the on-line computation problem. An elegant strategy developed in the last decade which includes an obstacle avoidance algorithm in the lowest level of control is the so-called potential field (or cost function) method, pioneered by Khatib [1] and studied by many others, e.g. [2–6]. The principle idea is to construct a suitable potential field with an attractive global minimum at the goal point and repulsive local maxima at the obstacles. Motion is guided by forces along the associated gradient. The desired characteristics of a potential field are the absence of local minima representing stable equilibrium points, a low computational burden and reasonably short trajectories to the goal point.

However, some of the previously developed potential functions may exhibit local minima even for only one obstacle in the workspace [7], which means that the system may terminate its operation prematurely. Attempts to eliminate local minima were discussed in [2] and include *navigation functions* [6] and *elliptical* [8] and *superquadratic* [9,7] artificial potentials. These approaches gradually transform the shapes of attractive and repulsive potentials in order to construct a combinational potential field without the generation of local minima, or at least with only "spurious minima" [7]. It was shown by Rimon and Koditschek (see e.g. [2,6]) that there always exists a suitable potential function for a class of "star-shaped"† obstacles. Using diffeomorph mappings, the "star-shapes" are transformed into discs in a "model sphere world" in which the potential function then is constructed [6]. However, such additional procedures increase the required computation time and thus decrease the attractiveness of the potential function method as an efficient and elegant on-line approach. In addition to these analytical potential functions, discrete methods were proposed, e.g. a numerical solution to the boundary problem of Laplace's equation [10] and numerical simulation of an unsteady diffusion process [11]. A numerical strategy has the inherent disadvantage that the potential field has to be calculated for each point of a large part of the workspace.

Given a planned path, the next step is to design a motion controller to track the gradient or force lines of the potential function without colliding with the obstacles. In almost all of the previous work, the artificial potential was coupled into the motion dynamics, effectively applying a control force along the gradient lines of the potential function [1,9]. Obviously, this does not lead to motion *along* the gradient lines; however, it was claimed that collisions with the obstacles are avoided since the repulsive potential goes to infinity at the obstacle boundaries. In addition to computational difficulties, this approach fails to specify the resulting system behavior and motion trajectories in the presence of actuator limitations. Consequently, the desired trajectories, represented by the gradient lines, are approached asymptotically [12] and no effective guarantee is given to avoid collisions under all circumstances during the transient phase. A first attempt considering the dynamics of the system was presented in [13], where the state velocity was included in the construction of a "generalized" potential field. In [3], the direction of the resultant force (sum of attractive and repelling potential) was used as the steering command input.

In this paper, a generalized harmonic function is used as a potential field [14,15], which exhibits no undesired local minima by nature. We propose to interpret the gradient lines as the **desired system trajectories**, rather than implementing a dynamic relation between the robot and its environment [16]. We design a sliding mode controller to provide motion *along* the gradient lines of the potential field. In contrast to the nonlinear feedback approach requiring exact knowledge of the robot dynamics [1,12], the sliding mode approach compensates for uncertainties and disturbances in the system. In a case study, we examine the motion of a mobile robot in 2D operating in an environment obstructed by several obstacles. Our method is *global* in the sense that it assumes a priori knowledge of the robot workspace and results in *reasonably* short trajectories to the goal point. It has also a *local* aspect, since it only considers the obstacle closest to the present location. The proposed path control algorithm is illustrated in several simulations. The underlying principle can be extended to strategies for partially known environments, based on a combination of a priori knowledge and local sensor information of the environment. The proposed strategy is expected to yield similar results in higher dimensional spaces like the configuration space of robotic manipulators.

2 Problem Statement and Dynamic Model

This paper addresses the problem of controlling the motion of an autonomous system from some initial point to a specified end point. The trajectory should be generated to avoid collisions of the mechanical system with its environment. The general idea is applicable to problems of arbitrary dimension, e.g. mobile robots in 2D or 3D and n-link manipulators in configuration space. The method is illustrated with a planar mobile robot to be navigated to a specified goal point without colliding with obstacles.

†A "star-shaped" set has a distinct center point from which all rays cross their boundary once and only once [6].

The general dynamic model of an mechanical system is given by

$$M(x)\ddot{x} + f(x,\dot{x}) = u, \tag{1}$$

where $x \in \mathbf{R}^n$ describes the system state (i.e. position of a mobile robot with respect to a fixed reference coordinate system, or joint displacements of a robot manipulator), $M(x) \in \mathbf{R}^{n\times n}$ is a mass or inertia matrix, $f(x,\dot{x}) \in \mathbf{R}^n$ comprises centripedal, Corriolis, gravitational effects and additive disturbances, and $u \in \mathbf{R}^n$ are mechanical control forces.

We assume that the Euclidean norm (denoted by $\|\cdot\|$ throughout the paper) of the term $f(x,\dot{x})$ is bounded over the range of operating conditions $(x,\dot{x})$ by a known scalar constant

$$\|f(x,\dot{x})\| \leq \bar{f}, \tag{2}$$

and that the mass/inertia matrix $M(x)$ is upper and lower bounded by

$$\underline{m}\|y\|^2 \leq y^T M(x) y \leq \bar{m}\|y\|^2, \tag{3}$$

where $\underline{m} = \lambda_{\min}\{M(x)\}$, $\bar{m} = \lambda_{\max}\{M(x)\}$, and an arbitrary vector $y \in \mathbf{R}^n$.

3 Motion Control Based on Sliding Mode

In this section we design a sliding mode controller forcing the mechanical system (1) to follow the gradient lines of an arbitrary artificial potential field. Sliding mode control is widely used in linear and nonlinear systems, in particular in robotics. The basic idea is to force the dynamic system to restrict its motion to a manifold called the sliding surface. The main benefits of sliding mode are its invariance properties and its ability to decouple high dimensional problems into sub-tasks of lower dimensionality. The interested reader is referred to [17] for a tutorial introduction and to [18,19] for a more detailed discussion of sliding mode theory.

Most previous implementations of artificial potential fields apply forces along the gradient, which amounts to specifying a *reasonable* system behavior without specifying the system trajectories [16]. Tracking controllers (see e.g. [12]) designed to remedy this problem depend on exact knowledge of the system dynamics and the equation of the desired trajectory. The proposed sliding mode controller provides tracking of the gradient lines after a finite transient, based only on knowledge of the momentary gradient, and is robust with respect to uncertainties and disturbances in the motion equation (1).

The key idea is to regard the state velocity rather than the state acceleration as the variable under control. The n-dimensional sliding manifold is defined as

$$s = \dot{x} + v_d(t)\frac{\mathrm{grad}U}{\|\mathrm{grad}U\|} = 0, \tag{4}$$

with the scalar "desired" velocity $v_d(t)$ being given by

$$v_d(t) = \min\left(v_0\,,\, k_v d(t)^{\frac{1}{2}}\right), \tag{5}$$

where v_0 is the desired standard velocity, $d(t)$ is Euclidian norm of the distance to the goal point, k_v is a scalar gain depending on the system deceleration capabilities, and $U(x)$ is a scalar potential function for $x \in \mathbf{R}^n$ to be defined later.

The restriction of the system to the manifold (4) simply means that the state velocity vector $\dot{x}$ is directed along the negative gradient of $U(x)$ with its magnitude being specified in (5).

The "traveling" velocity v_d and the normalization of the gradient provide boundedness of the control. Furthermore, a proper choice of k_v prevents "overshoot" at the goal point and at the same time guarantees a finite approach [14]: Provided sliding mode occurs, the state velocity will be colinear to $(-\mathrm{grad}U)$ in a vicinity of the goal point. Therefore, the motion equation (1) is restricted to the manifold (4) and can be reduced to a description of the scalar distance to the goal point:

$$\dot{d}(t) = -k_v d(t)^{\frac{1}{2}}. \tag{6}$$

The solution of (6)

$$d(t) = \left(-\frac{k_v t}{2} + d(0)^{\frac{1}{2}}\right)^2 \tag{7}$$

vanishes after a finite time interval:

$$d(t) \equiv 0 \quad for \quad t \geq \frac{2}{k_v} d(0)^{\frac{1}{2}}. \tag{8}$$

To ensure the existence of sliding mode in the manifold $s = 0$ given in (4), we examine the *Lyapunov function* candidate

$$V = \frac{1}{2}s^T s. \tag{9}$$

Differentiating (9) along the motion trajectories (1) yields

$$\dot{V} = s^T\left(M(x)^{-1}u + F(t)\right) \tag{10}$$

where

$$F(t) = -M(x)^{-1}f(x,\dot{x}) + \dot{v}_d(t)\frac{\mathrm{grad}U}{\|\mathrm{grad}U\|} + v_d(t)\frac{d}{dt}\left(\frac{\mathrm{grad}U}{\|\mathrm{grad}U\|}\right). \tag{11}$$

Given the bounds on $f(x,\dot{x})$ in (2) and $M(x)$ in (3), a standard approach is to enforce sliding mode along the manifold $s = 0$ (4) in the domain where

$$\dot{v}_d(t)\frac{\mathrm{grad}U}{\|\mathrm{grad}U\|}, \quad \text{and} \quad \frac{d}{dt}\left(\frac{\mathrm{grad}U}{\|\mathrm{grad}U\|}\right) \tag{12}$$

are bounded by using the "unit" control [20,21]

$$u = -u_0\frac{s}{\|s\|}, \tag{13}$$

where u_0 is the available control force. For arbitrary actuator constraints, the method presented in [22] can be utilized.

Substituting (13) into (10) results in

$$\dot{V} \leq \|s\|\left(-\frac{u_0}{\bar{m}} + \|F\|\right). \tag{14}$$

It follows from (14) that $\dot{V} < 0$ for some finite value of u_0, which implies convergence to the manifold $s = 0$. The time interval needed for convergence is *finite* and can be adjusted by choosing an appropriate magnitude of control. Consequently, in contrary to conventional approaches with the control force being colinear to the gradient, the bounded control (13) leads to ideal tracking of the desired trajectories delineated by the gradient lines of the potential function.

A crucial issue are the boundedness assumptions in (12). Under the assumption that sliding mode occurs during the approaching phase (6) differentiation of $v_d(t) = k_v d(t)^{\frac{1}{2}}$ leads to

$$|\dot{v}_d(t)| = \frac{1}{2}k_v^2. \tag{15}$$

Furthermore, it is of interest to note that, although $\frac{\mathrm{grad}U}{\|\mathrm{grad}U\|}$ is bounded, $\frac{d}{dt}\left(\frac{\mathrm{grad}U}{\|\mathrm{grad}U\|}\right) = \frac{\partial}{\partial x}\left(\frac{\mathrm{grad}U}{\|\mathrm{grad}U\|}\right)\dot{x}$ may become unbounded. Physically, this simply means that the curvature of the gradient field should be bounded to enable tracking with finite control, which is equivalent to finite acceleration.

The control force defined in (13) is discontinuous at $s = 0$ and thus not feasible with real-life actuators due to their inertia, which may result in chattering. An efficient tool to overcome this problem is to use asymptotic nonlinear observers [23].

4 Harmonic Laplacian Potential Field

In the following sections, we will discuss the design of the potential field U already mentioned in the previous section. It was proposed in [14,15] to use an electrostatic field as an artificial potential function to specify the desired trajectories. The main advantage of a Coulomb potential is the implicit absence of local minima, which would generate stable equilibrium points at undesired locations. Per definition, all force lines begin and terminate either at a positive or negative charge or at infinity. The standard Coulomb potential in $\mathbf{R}^3$ is characterized by its harmonic (Laplace-) property

$$\nabla^T\cdot\nabla U(x) = \sum_{i=1}^{3}\frac{\partial^2 U(x)}{\partial x_i^2} = 0, \quad x = (x_1,x_2,x_3). \tag{16}$$

The Laplace equation (16) is a direct consequence of the Maxwell equations applied to a static electrical field and is also known as the Gaussian property

$$\mathrm{div}\vec{E} = \mathrm{div}\cdot\mathrm{grad}U = 0. \tag{17}$$

Geometrically, (16) means that the balance of gradient lines entering and leaving any closed surface in the domain in which the potential field is defined is proportional to the charges enclosed by the surface. In other words, potential maxima and minima do not exist away from the charges.

In [15], the standard Coulomb potential for point charges was extended to the n-dimensional Euclidean space by solving the Laplace equation (16) in the open domain $r > 0$ with (see also [4])

$$r = \left(\sum_{i=1}^{n} x_i^2\right)^{\frac{1}{2}}, \quad x = (x_1, x_2, ..., x_n). \tag{18}$$

The generalized harmonic potential of a point charge[‡] C is given by

$$U(r) = \begin{cases} \frac{C}{r^{n-2}} & n = 1, 3, 4, ... \\ C \ln \frac{1}{r} & n = 2. \end{cases} \tag{19}$$

The associated "electrostatic" force field is found by

$$E(r) = -\text{grad}U(r) = \begin{cases} (n-2)\frac{C}{r^{n-1}} & n = 1, 3, 4, ... \\ \frac{C}{r} & n = 2. \end{cases} \tag{20}$$

It is easy to show that all properties of the standard Coulomb field for $\mathbf{R}^3$, and in particular the superposition principle, are preserved.

The gradient of the potential field to be designed should have the following characteristics:

1. No gradient lines should be directed *into* the "forbidden" zone around each obstacle. In other words, at any point on the boundary of this zone, the gradient should be directed *away* from the obstacle.
2. The resulting "desired" trajectories should be reasonably short.
3. The curvature of the gradient lines should be bounded (12) to enable tracking with finite control (13) while maintaining some constant velocity.
4. The gradient field has to be easy to compute with regard to on-line implementation in systems with arbitrary degree–of–freedom as relevant for robotic manipulator control in configuration space.

5 Case Study: Mobile Robot in the Plane

5.1 Robot Dynamics and Environment Model

In this section, we discuss the planar path control problem for a mobile robot. A point autonomous robot is used as a simplified abstract model for real-life roving robots designed for fast motion:

$$m\ddot{x} + f(x, \dot{x}) = u, \tag{21}$$

where $\underline{m} \leq m \leq \bar{m}$ represents the point mass, $\|f(x, \dot{x})\| \leq \bar{f}$ comprises the uncertainty in the system, $x(t) \in \mathbf{R}^2$ denotes the location of the robot with respect to a fixed reference coordinate system and $u \in \mathbf{R}^2$ is the control input. For simplicity, the rotational degree of freedom of the mobile robot is neglected here. The algorithm can be easily modified to account for specific robot dynamics.

Each obstacle in the workspace is covered by an elliptical "security zone". Each obstacle is "grown" by the maximum size of the automaton to account for the physical dimension of a real-life robot. In order to preserve as much space as possible for admissible motion, the location, orientation and the size of each "security ellipse" should be minimized. We use a simple coordinate transformation to map the elliptical zone into a circle [24]. It should be noted that it is also possible to map more complex obstacle security zones into circles in $\tilde{x}$-space, using conform mappings as frequently found in the field of fluid dynamics [4,5], or using the "star-shape"–to–circle diffeomorph mapping described in the works of Rimon and Koditschek, see e.g. [6]. A potential field is constructed based on the new coordinate system $\tilde{x} = Tx$, and the resulting gradient field is then transformed back into the original coordinate system x. In the sequel, we will confine the development to circular security zones with radius R.

5.2 Potential Field Design

In the construction of an artificial electrical field (19), it was proposed in [14] to model a negative unit charge in the goal point and a distributed positive charge in the obstacles. Given that the total positive charge is *less* than unity, all gradient lines will begin either at the obstacle or at infinity and *all* lines will terminate in the goal point. However, the calculation of the field created by a distributed charge is rather tedious. [4] uses the equivalent of line charges in an interpretation of the Laplace equation as an incompressible flow. Heuristics are introduced to overcome "structural minima" arising from the combination of attractive and repelling potentials. In [15], a positive point charge in each obstacle is considered. The need to prevent the gradient lines from intersecting the "forbidden" regions around the obstacles leads to a mathematical programming problem in order to determine suitable magnitudes of the point charges, a procedure which requires substantial pre-computations.

In order to facilitate the on-line computations in clustered environments we propose to construct the harmonic Laplacian potential field using only the goal point and the obstacle closest to the present location of the point robot. This requires to "switch" the potential function whenever another obstacle gets closer than the one presently being considered. The regions in which a specific obstacle is being considered at a certain time instance can be determined a priori and stored in a simple "look-up" table that also contains the necessary geometric information about the respective obstacle. It is shown later in the development that this "switching" indeed results in "well-behaved" motion when passing between two obstacles andobviously yields a low computational burden. Consequently, the following discussion is based on a configuration with a single obstacle. In the design of the "electrical" potential field, we place a negative unit charge at the goal point and a positive charge $q < 1$ in the obstacle closest to the position of the

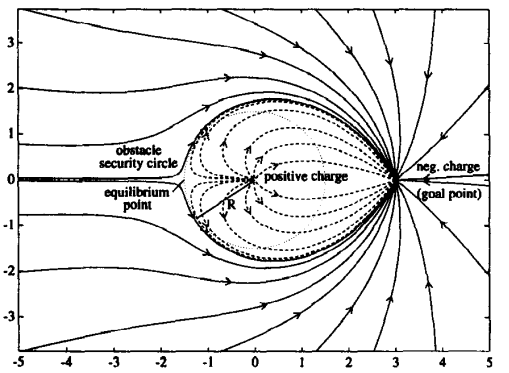

Figure 1: Gradient field of an electrical potential field created by one positive charge in the circle center and one negative charge in the goal point

point mass. It is evident that the resulting gradient field has only one equilibrium point[§] which lies on a straight line through the two charges. It is easy to show that this equilibrium point is *unstable*. In the following we will illustrate how to choose the positive point charge q such that the gradient lines of the resulting potential field fulfill the required properties.

A primary concern is to construct the potential field such that the gradient line do not cross the obstacle boundary from "outside–to–inside" (Property 1). We propose to "place" the equilibrium point at the boundary of the security circle.

Theorem 1.

Consider a two charge system in the plane consisting of a negative unit point charge and a positive point charge $q < 1$. If

$$q = \frac{R}{R + D} \tag{22}$$

where $R > 0$ is the radius of a circle around the positive point charge and $D > 0$ is the distance between the two charges, then all gradient lines of the planar harmonic potential (19) are directed away from the positive point charge inside the circle. □

In order to ensure steady motion towards the obstacle we show that the gradient lines defined in (31) and (32) have always a component directed towards the goal point (Property 2).

Theorem 2.

Consider a two charge system similar to Figure 1. If q is as defined in (22), then the gradient of the planar potential U given in (19) is always directed towards the goal point except inside a circle of radius R around the positive point charge. □

The proofs Theorems 1 and 2 are given in the Appendix.

[‡] Also the term "electric field" has no physical meaning in $\mathbf{R}^n$ for $n \neq 3$, we will continue the use this terminology for convenience.

[§] We refer to points with $\text{grad}U = 0$ as equilibrium points.

It can be seen from Figure 1 that in the vicinity of the equilibrium point, the curvature of the gradient lines is high and in fact tends to infinity close at the equilibrium point. Consequently, tracking of the normalized gradient is not possible with finite control forces. To show this, let the equilibrium point be located at the origin of a Cartesian coordinate system, let the obstacle be at $(R,0)$ and the goal point at $(D,0)$. The "electrical" field (20) is given by

$$E = -\text{grad}U = \frac{R}{D}\begin{pmatrix} \frac{x-R}{(x-R)^2+y^2} \\ \frac{y}{(x-R)^2+y^2} \end{pmatrix} - \begin{pmatrix} \frac{x-D}{(x-D)^2+y^2} \\ \frac{y}{(x-D)^2+y^2} \end{pmatrix}. \quad (23)$$

For the sake of a qualitative illustration, we use a linearization around the equilibrium point $(0,0)$

$$\frac{\tilde{E}}{\|\tilde{E}\|} = \frac{D^2R}{R-D}\frac{1}{\sqrt{\delta x^2+\delta y^2}}\begin{pmatrix} -\delta x \\ \delta y \end{pmatrix}. \quad (24)$$

Direct differentiation of the desired motion equation

$$\dot{x} = v_d\frac{\tilde{E}}{\|\tilde{E}\|} \quad (25)$$

shows that the necessary acceleration tends to infinity when approaching the equilibrium point.

To remedy this problem, we propose to slow down the motion in the area of high curvature by modifying the sliding surface (4) as follows:

$$s = \dot{x} + v_d(t)\frac{\text{grad}U}{\max(\|\text{grad}U\|,\epsilon_U)}. \quad (26)$$

Provided ϵ_U is chosen appropriately, exact tracking of the gradient lines is guaranteed since the conditions (12) for sliding mode to exist along (26) are always fulfilled. The velocity is decreased automatically in the region where the curvature is high and the absolute value of the gradient is small.

Remark

The time needed to reach the goal might increase considerably for initial conditions very close to the "singular line" that goes through the obstacle center and the goal point. Such a situation should be prevented by introducing additional "forces" orthogonal to the singular line in its vicinity. However, any small perturbation will cause the mobile robot to leave this straight line without any additional modification. Figure 2 shows the motion trajectory with the starting point being very close to the singular line. It is of interest to note that "numerical" perturbations sufficed to cause the automaton to leave the singular trajectory.

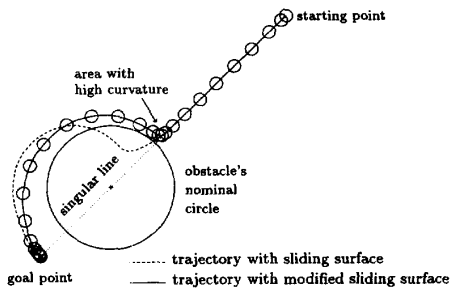

Figure 2: Motion trajectories with and without modified sliding surface

To improve the performance, i.e. to be able to maintain a constant velocity, heuristic measures should be taken to direct the motion away from the singular line. We propose to compensate the motion component towards the obstacle by modifying the security radius of the obstacle dynamically as follows:

$$R_s = \max\left(R - \frac{\dot{x}_r|\dot{x}_r|}{2\varepsilon_s a_{max}}, 0\right), \quad with \quad a_{max} = \frac{u_o - \bar{f}}{\sqrt{2}m}, \quad (27)$$

where R is the nominal radius of the obstacle being considered, $\dot{x}_r$ represents the radial velocity component directed towards the obstacle center ($\dot{x}_r$ is negative when approaching the obstacle), $\varepsilon_s \in (0,1]$ is a security factor that should be chosen close to 1, m is the mass of the point robot, u_0 is the available control force (13), and $\bar{f}$ is the bound on the system uncertainty (2). The obstacle charge q in (22) is adjusted according to (27).

Far away from the obstacle, the gradient field remains almost unchanged. However, when approaching the obstacle, the point mass is directed around the obstacle more smoothly in the sense that the tangential forces act "earlier" than without this modification (see Figure 3). On the other hand, the magnitude of the obstacle charge is decreased when the velocity component directed towards the obstacle decreases and the point mass moves "around" the obstacle. This ensures that the motion is not directed unreasonably far away from the obstacle. Moreover, if the trajectory leads away from the obstacle, the obstacle's charge even decreases below its nominal value. Thus the obstacle "charge" is chosen *as high as necessary* and *as low as possible*.

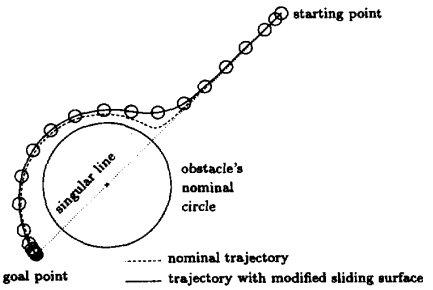

Figure 3: Nominal trajectory and motion with dynamic security circle modification

5.3 Multiple Obstacles

Until now we considered only one obstacle in the plane when constructing the potential field. In the case of multiple obstacles, our algorithm takes into account only the obstacle closest to the present location of the moving point mass. This requires to "switch" the potential field as the robot moves, creating a new "spatial" sliding surface. A pre-computed look-up table provides the necessary information which obstacle should be considered in a certain region, together with the geometric data about the obstacle's security zone. Naturally, the "time" sliding conditions (12) along (26) are violated at the switching points. Due to the characteristics of the proposed controller, the motion trajectories are adjusted to the *new* gradient lines as quickly as possible.

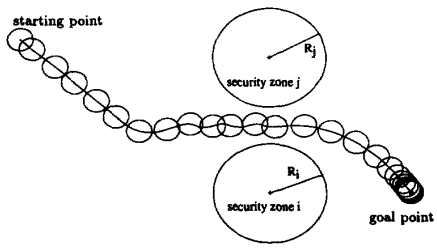

Figure 4: Motion trajectories in an environment with two obstacles

This ensures that passing between two obstacles located close to each other is achieved, in contrast to conventional approaches such as [1] and [25]. (See e.g. the comparison study in [26] and the derivations in [27] for detailed discussions of this problem). The disadvantage of the discontinuous gradient switching (see Figure 5.a) is that sliding mode of the real-world dynamic system cannot occur along the "time" sliding surface (4). This results in a "chattering"-like behavior (see Figure 4) in a boundary layer δ along the equi-distance line (or "spatial" sliding surface) between the two obstacle security zones.

To eliminate the chattering behavior, the gradient field should be switched "smoothly" using one of the standard continuous approximations for the step function frequently found in robust nonlinear controls literature. It should be noted that the approximation of the step function can be defined with respect to *time* as well as with respect to the *distance* to the charge switching line. In other words, in a boundary layer δ of the equi-distance line between the obstacles, the two closest obstacles contribute to the potential field with *time-dependent* or *state-dependent* weights.

Provided the "smooth" switching function is defined such that the curvature of the potential field does not exceed the maximal acceleration capability of the autonomous system at any point (see Figure 5.b), the sliding conditions (12) will not be violated when entering the boundary layer δ and sliding mode will continue along (26). This can be easily established by using the framework of equations (9-14).

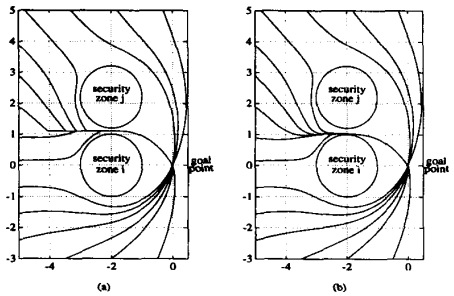

Figure 5: (a) Gradient field with discontinuous switch
(b) Gradient field with smooth switch

In the region where the gradients of each single field (i.e. one obstacle and the goal potential) are directed towards the equi-distance line, motion will occur in the boundary layer δ. Since the gradient of each obstacle/goal combination potential has a component directed towards the attractive goal point (see Theorem 2), the linear combination

$$\text{grad}U_{ij}^{*} = \mu_i \text{grad}U_i + \mu_j \text{grad}U_j, \qquad 0 < \mu_i < 1, \quad 0 < \mu_j < 1, \qquad (28)$$

has also a component directed towards the goal. It is of interest to note that formal application of Filippov's continuation method [28] leads to a similar result and implies that $\mu_i + \mu_j = 1$ within the boundary layer δ. Although the equi-distance line will not be followed exactly, the motion trajectory will exhibit no chattering, since the gradient lines now are smooth with bounded curvature.

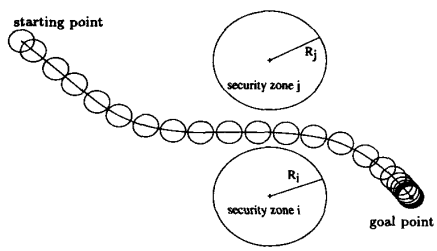

Figure 6: Motion trajectories in an environment with two obstacles using a continuous approximation for the charge switching function

For illustration purposes, we simulate the system in an environment similar to the one shown in Figure 4, using a piecewise linear approximation of the step-function for the charge switching. Numerical results for this example are shown in Figure 6. When passing between the obstacles i and j, the potential changes "smoothly"

$$\text{grad}U_{ij}^{*} = \begin{cases} \text{grad}U_i & \text{for} \quad \varrho < -\frac{\delta}{2}, \\ \mu \text{grad}U_i + (1-\mu)\text{grad}U_j & \text{for} \quad |\varrho| < \frac{\delta}{2}, \\ U_j & \text{for} \quad \varrho > \frac{\delta}{2}, \end{cases} \qquad (29)$$

where ϱ is the distances to the equi-distance line $s_{equi} = 0$ (counted positive on the "side" of obstacle j), and $\mu = \frac{1}{2} + \frac{\varrho}{\delta}$. In this case, U_{ij}^{*} is state dependent and has a bounded derivative, which ensures that "time" sliding mode exists along (26).

Navigation through a narrow path between two obstacles without collisions can be achieved along a smooth path due to the ideal tracking properties of the *sliding mode controller*. A more detailed discussion of the problems attributed to the potential field method [27] for the navigation through narrow passages can be found in [29]. Figure 7 shows the motion trajectory of a circular robot in an environment with three obstacles approximated by ellipses. Different ellipse–to–circle transformations were utilized for each obstacle.

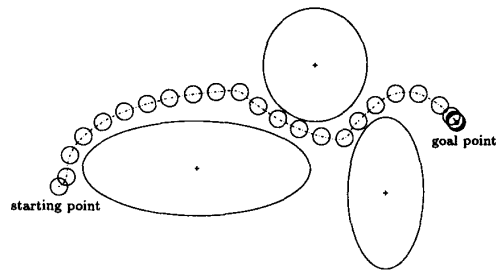

Figure 7: Motion trajectory in an environment with three obstacles

6 Conclusions

In this paper we introduced a sliding mode controller for n-dimensional mechanical systems that guarantees exact tracking of the gradient lines of an artificial potential field in spite of uncertainties. In contrast to conventional approaches which apply forces along the gradient of the potential field, the system velocity is oriented along the gradient and the motion trajectories thus coincide with the gradient lines. This opens completely new perspectives for path control (integrated path planning and motion control) using the potential field method both in *global* and *local* problems. The design problem is simplified to constructing a potential field such that all gradient lines lead to the goal point and do not cross the obstacle boundaries.

The strategy is applied to mobile robots operating in an environment with known obstacles. A planar harmonic potential with the above properties is presented which avoids the problems previously encountered in potential fields, e.g. local minima. Only the closest obstacle is considered at each time instance. When passing between two obstacles, the switching of the associated gradient fields leads to a new, "spatial" sliding surface. Smooth motion is achieved by introducing time-dependent or state-dependent approximations of the gradient field switching to enable "time" sliding mode to occur, i.e. to be able to track the gradient lines with finite control efforts. Due to its low computational complexity, the method shows promising perspectives for implementation in unknown and partially known environments (i.e. a sensor-based path control) and for spaces of higher dimensions, e.g. for robot manipulators in n-dimensional configuration space.

Acknowledgements

The authors would like to thank Prof. J. Ackermann of DLR, Germany, for his support and encouragement of this work.

Appendix

Proof of Theorem 1
We will base the argument on the situation shown in Figure 1. The obstacle center is located at the origin and the goal point at a distance D from it. The potential at some point (r, φ) with respect to a polar coordinate system is given by

$$U(r,\varphi) = q \ln\left(\frac{1}{r}\right) - \frac{1}{2}\ln\left(\frac{1}{r^2 - 2Dr\cos\varphi + D^2}\right), \qquad (30)$$

thus, the gradient field is

$$E_r(r,\varphi) = -\frac{\partial U(r,\varphi)}{\partial r} = \frac{q}{r} - \frac{r - D\cos\varphi}{r^2 - 2Dr\cos\varphi + D^2}, \qquad (31)$$

$$E_\varphi(r,\varphi) = -\frac{1}{r}\frac{\partial U(r,\varphi)}{\partial \varphi} = -\frac{Dr\sin\varphi}{r^2 - 2Dr\cos\varphi + D^2}. \qquad (32)$$

The equilibrium point is located on the boundary of the circle since $E_r = E_\varphi = 0$ at $r = R$, $\varphi = \pi$. Therefore we refer to this choice of the charge q (22) as an "equilibrium point placement" method. Since we want to determine the area where $E_r > 0$, we have to examine the points where $E_r = 0$. The loci $E_r = 0$ correspond to an equi-potential line that necessarily forms a closed curve. Due to geometric considerations, this curve must encircle the origin. In the vicinity of the origin, $E_r > 0$. We now show that the obstacle's forbidden circle lies inside the curve $E_r = 0$ provided q is chosen according to (22). As a consequence, $E_r > 0$ in the entire circle. Solving

$$E_r(r,\varphi) = \frac{q}{r} - \frac{r - D\cos\varphi}{r^2 - 2Dr\cos\varphi + D^2} \equiv 0 \qquad (33)$$

for $\left(\frac{r}{R}\right)$ with $\alpha=\frac{D}{R} > 0$ yields

$$\left(\frac{r}{R}\right) = \frac{1}{2}\cos\varphi(\alpha-1) \pm \sqrt{\frac{1}{4}\cos^2\varphi(\alpha-1)^2+\alpha}. \quad (34)$$

Since $r>0$ and $0<\varphi<2\pi$, we only consider the solution of (34) with the positive sign. Due to $a \geq 1$ (the goal point has to lie outside the obstacle!),

$$r \geq R \qquad \forall\varphi \in [0;2\pi) . \quad (35)$$

As a consequence of (35), $E_r > 0$ inside the circle with $r < R$. In fact, this is also true for the boundary $r = R$ except for the point located directly opposite the negative charge where $E_r = 0$. □

Proof of Theorem 2

To facilitate the analysis, the goal point is now placed in the origin, while the obstacle center is located at a distance D from the goal.

The potential function for the two charge system is given by

$$U(r,\varphi) = \frac{q}{2}\ln\left(\frac{1}{r^2-2Dr\cos\varphi+D^2}\right) - \ln\frac{1}{r}. \quad (36)$$

In following a similar procedure as in the proof of Theorem 1, we examine the points where $E_r(r,\varphi)=0$ and show that $E_r < 0$ everywhere except inside the obstacle's security circle. Solving

$$E_r(r,\varphi) = q\left(\frac{r-D\cos\varphi}{r^2-2Dr\cos\varphi+D^2}\right) - \frac{1}{r} \equiv 0 \quad (37)$$

for $\cos\varphi$ yields

$$\cos\varphi = \frac{r^2+\alpha(\alpha+1)R^2}{Rr(1+2\alpha)}, \quad (38)$$

where $\alpha = \frac{D}{R}$. Due to the constraint $|\cos\varphi| \leq 1$, this gives the following condition for r:

$$D \leq r \leq D+R. \quad (39)$$

The "security circle" with radius R around the obstacle is given in polar coordinates by

$$r^2 - 2\alpha Rr\cos\varphi + \alpha^2R^2 \leq R^2. \quad (40)$$

To show that the curve $E_r(r,\varphi)=0$ lies inside this circle, we equate the right-hand side of (40) along (38):

$$r^2 - 2\alpha Rr\cos\varphi + \alpha^2R^2 = \frac{1}{1+2\alpha}(r^2-\alpha^2R^2) \leq R^2, \quad (41)$$

where the left side of the inequality (39) has been used to reduce the expression.

Since $E_r < 0$ far away from charges for $q < 1$, (41) shows that the gradient is directed towards the goal point everywhere outside the obstacle security circle. □

References

[1] O. Khatib, "Real-time obstacle avoidance for manipulators and mobile robots," *Int. Journal of Robotics Research*, vol. 5, no. 1, pp. 90–98, 1986.

[2] D. E. Koditschek, "Exact robot navigation by means of potential functions: Some topological considerations," in *Proc. IEEE Conf. on Robotics and Automation*, (Raleigh, NC, USA), pp. 1–6, 1987.

[3] J. Borenstein and Y. Koren, "Real-time obstacle avoidance for fast mobile robots," *IEEE Trans. on Systems, Man, and Cybernetics*, vol. 19, no. 5, pp. 1179–1187, 1989.

[4] J.-O. Kim and P. Khosla, "Real-time obstacle avoidance using harmonic potential functions," in *Proc. IEEE Conf. on Robotics and Automation*, (Sacramento, CA, USA), pp. 790–796, 1991.

[5] D. Megherbi and W. A. Wolovich, "Real-time velocity feedback obstacle avoidance via complex variables and conformal mapping," in *Proc. IEEE Conf. on Robotics and Automation*, (Nice, France), pp. 206–213, 1992.

[6] E. Rimon and D. E. Koditschek, "Exact robot navigation using artificial potential functions," *IEEE Trans. on Robotics and Automation*, vol. 8, no. 5, pp. 501–518, 1992.

[7] P. Khosla and R. Volpe, "Superquadratic artificial potentials for obstacle avoidance and approach," in *Proc. IEEE Conf. on Robotics and Automation*, (Philadelphia, PA, USA), pp. 1778–1784, 1988.

[8] R. Volpe and P. Khosla, "Artificial potentials with elliptical isopotential contours for obstacle avoidance," in *Proc. IEEE Conf. Decision and Control*, (Los Angeles, CA, USA), pp. 180–185, 1987.

[9] R. Volpe and P. Khosla, "Manipulator control with superquadratic artificial potential functions: Theory and experiments," *IEEE Trans. on Systems, Man, and Cybernetics*, vol. 20, no. 6, pp. 1423–1436, 1990.

[10] C. I. Connolly and J. B. Burns, "Path planning using Laplace's equation," in *Proc. IEEE Conf. on Robotics and Automation*, (Cincinati, OH, USA), pp. 2102–2106, 1990.

[11] G. Schmidt and K. Azarm, "Mobile robot navigation in a dynamic world using an unsteady diffusion equation strategy," in *Proc. IEEE/RSJ Int. Conf. on Intelligent Robots and Systems*, (Raleigh, NC, USA), 1992.

[12] D. E. Koditschek, "Some applications of natural motion control," *ASME Journal of Dynamic Systems, Measurement and Control*, vol. 113, pp. 552–557, 1991.

[13] B. H. Krogh, "A generalized potential field approach to obstacle avoidance control," in *Proc. SME Conf. on Robotics Research*, (Bethlehem, PA, USA), 1984.

[14] V. I. Utkin, S. Drakunov, H. Hashimoto, and F. Harashima, "Robot path obstacle avoidance control via sliding mode approach," in *Proc. IEEE/RSJ International Workshop on Intelligent Robots and Systems*, (Osaka, Japan), pp. 1287–1290, 1991.

[15] H. Hashimoto, F. Harashima, V. I. Utkin, S. A. Krasnova, and I. M. Kaliko, "Sliding mode control and potential fields in obstacle avoidance," *Proc. European Control Conference*, pp. 859–862, 1993.

[16] N. Hogan, "Impedance control: An approach to manipulation: Parts I-III," *ASME Journal of Dynamic Systems, Measurement and Control*, vol. 107, pp. 1–24, 1985.

[17] R. A. DeCarlo, S. H. Żak, and G. P. Matthews, "Variable structure control of nonlinear multivariable systems: A tutorial," *Proceedings of the IEEE*, vol. 76, no. 3, pp. 212–232, 1988.

[18] V. I. Utkin, *Sliding Modes in Control and Optimization*. Berlin, Germany: Springer-Verlag, 1992.

[19] A. S. I. Zinober, ed., *Deterministic control of uncertain systems*. London, UK: P. Peregrinus Ltd., 1990.

[20] E. P. Ryan and M. Corless, "Ultimate boundedness and asymptotic stability of a class of uncertain systems via continuous and discontinuous feedback control," *IMA Journal of Math. Cont. and Info.*, vol. 1, pp. 223–242, 1984.

[21] C. M. Dorling and A. S. I. Zinober, "Two approaches to hyperplane design in multivariable variable structure control systems," *Int. Journal of Control*, vol. 44, no. 1, pp. 65–82, 1986.

[22] S. Baida, "Unit sliding mode control in continuous and discrete time systems," *Int. Journal of Control (special issue on Sliding Mode Control)*, vol. 56, 1993.

[23] A. G. Bonadrev, S. A. Bondarev, N. E. Kostyleva, and V. I. Utkin, "Sliding modes in systems with asymptotic state observers," *Automation and Remote Control*, vol. 46, no. 6 (P.1), pp. 679–684, 1985.

[24] B. J. Oommen and I. Reichstein, "On translating ellipses amidst elliptical obstacles," in *Proc. IEEE Conf. on Robotics and Automation*, (San Fransisco, CA, USA), pp. 1755–1760, 1986.

[25] M. Okutomi and M. Mori, "Decision of robot movement by means of a potential field," *Advanced Robotics*, vol. 1, no. 2, pp. 131–141, 1986.

[26] H. Noborio, S. Wazumi, and S. Arimoto, "An implicit approach for a mobile robot running on a force field without generation of local minima," *in Preprints of the 11th IFAC Congress*, (Tallin, USSR), pp. 85–90, 1990.

[27] Y. Koren and J. Borenstein, "Potential field methods and their inherent limitations for mobile robot navigation," in *Proc. IEEE Conf. on Robotics and Automation*, (Sacramento, CA, USA), pp. 1398–1404, 1991.

[28] A. F. Filippov, "Application of the theory of differential equations with discontinuous right-hand sides to non-linear problems of automatic control," in *Proc. of the 1st IFAC Congress, vol. II*, (Butterworths, London, UK), pp. 923–927, 1961.

[29] J. Guldner and V. I. Utkin, "On the navigation of mobile robots in narrow passages: A general framework based on sliding mode theory," Tech. Rep. 515-93-17, DLR, Germany, 1993.